Modelling and Control of a Cascaded Doubly-Fed Induction Generator based on Dynamical Equivalent Circuits

N. Patin, *Member, IEEE,* E. Monmasson, *Senior Member, IEEE,* J.-P. Louis

***Abstract*— This paper deals with the control of an autonomous cascaded doubly-fed induction generator operating in a variable speed constant frequency mode. The proposed structure is a full stand-alone generating system dedicated to isolated grids in embedded systems or in small scale renewable energy systems such as windmill and hydropower generators. The study is focused on the CDFIG. Its behaviour against several design parameters (numbers of pole pairs and rotor interconnexion) is recalled. A model, based on dynamical equivalent circuits, is also given for the design of the controller. Finally, the synthesized controller is validated by simulations and experimental results.**

***Index Terms*— Cascaded Doubly-Fed Induction Generator, Variable Speed Constant Frequency, Isolated grid, Aircraft applications, Topology analysis, Modelling, Control.**

I. INTRODUCTION

THE electrical consumption has dramatically increased in the last decades both in stationary and mobile applications. In these two cases, constant frequency AC grids are used whereas primary mechanical power sources usually operate at variable speed. Thus, an adapted architecture of generating systems is required. Constant frequency voltages cannot be directly provided by synchronous generators, which must be associated to rectifier/inverter sets in such systems. The only kind of electromechanical generator, operating at variable speed, which can be directly connected to a constant frequency grid is the doubly-fed induction machine (DFIG): indeed, they are used in small scale generators in windmills for instance. However, specific applications can require high level reliability and/or long-time maintenance periodicity. So, on the basis of these constraints, Cascaded Doubly-Fed Induction Generator (CDFIG) is a good candidate for DFIG replacement because of its similar behaviour without brushes and sling rings which are the main drawback of this machine (notice that CDFIG has been already studied in various applications such as windmills [1], small-scale hydropower [2] and aicraft power supply [3]).

This association of two Doubly-Fed Induction Machines (DFIM), mechanically and electrically coupled, can be justified on the basis of a functional inversion principle and the constraint forbidding sliding contacts in targeted applications. This synthesis methodology will be developed in the following section (section II). Then, three parameters can be identified in the CDFIG:

- Number of pole pairs p_1 of the first DFIM (DFIM1),
- Number of pole pairs p_2 of the first DFIM (DFIM2),
- Electrical coupling sequence between rotor windings of the two machines (two cases: direct and inverse coupling sequences characterized using a coefficient $\lambda_c = +1$ and $\lambda_c = -1$ respectively).

These three parameters have a significant impact on the behaviour of the CDFIG and a rigorous analysis (using ideal models of DFIMs) is then required in order to identify the best configuration(s). This is the aim of section II and it allows to describe the power flow through the two machines in order to evaluate qualitatively the generator efficiency (section IV). Finally, it will be also possible to discuss on complementary constraints related to the CDFIG design for an integration of the two machines into a single frame [4].

Then, even if CDFIG modelling (section IV) is as generative as possible, it is oriented by preliminary results, more particularly concerning coupling sequence between rotor windings. So, a model of a realistic generator is established using a graphical representation of the system, adapted to the end-user point of view: an electrical scheme. The representation proposed in this paper (*dynamical equivalent circuit* representation) is not limited to the classical case of sinusoidal steady-state operation but it can be applied to a transient description of the system. Then, this model is used for the design of the CDFIG controller, based on the model inversion principle which will be detailed in section V.

Finally, all this study is illustrated by simulations and experimental results (section VI) being based on a test bench developed in our laboratory. All the parameters of this experimental set-up have been used in simulation using Matlab/Simulink and the proposed controller has been validated and implemented in a real-time controller board dSpace DS1104.

II. ARCHITECTURE SYNTHESIS

An architecture of electrical generator can be synthesized using a functional inversion methodology: the only variables which are initally defined are the outputs of the system. In the case studied here, a constant frequency output voltage is wanted. Thus, due to the inductive behaviour of induction (and synchronous) machines, parallel capacitors connected to the grid are required. Then, a variable speed constant frequency (VSCF) generator must be introduced because of speed variations of the prime mover in such applications. A good candidate for VSCF operation is the well-known doubly-fed induction machine (DFIM) because stator frequency can be maintained constant in spite of speed variations thanks to

opposite variations of the rotor frequency, controlled by a Voltage Switching Inverter (VSI). This classical structure, which is currently used in windmills is not completely adapted in the aircraft environment due to slip rings in the DFIM, prohibited in this case. So, another solution must be investigated.

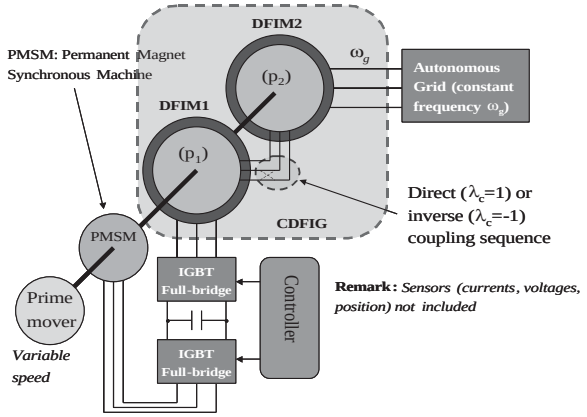

Fig. 1. Full stand-alone generator based on two cascaded Doubly-Fed Induction Machines (DFIMs)

If the DFIM is conserved, rotor windings must be supplied by another three-phase AC machine: another DFIM is introduced as it is shown in Fig. 1. It can be seen that these two doubly-fed inductions machines can be directly connected and finally integrated, giving us a complete brushless solution called Cascaded Doubly-Fed Induction Machine – CDFIM (more precisely here Generator – CDFIG). Notice that the global structure of the generator based on a single doubly-fed induction generator can be conserved with the CDFIG: the stator windings of the DFIM n°1 are connected to a VSI and this inverter is supplied by a PWM rectifier connected to a Permanent Magnet Synchronous Machine (PMSM) allowing full stand-alone capabilities to the complete VSCF generator.

The study presented in the following section is focused on the CDFIG. Indeed, it is necessary to analyse the behaviour of this structure with respect to its main parameters (p_1, p_2 and λ_c):

III. CDFIG ANALYSIS

This study is based on a simplified model of the doubly-fed induction machine where copper/iron losses and magnetic leakages are neglected. Thus, a DFIM is characterized by the following equations

$$\begin{cases} \omega_s = \omega_r + p\Omega \\ P_r = -s.P_s \\ P_s + P_r = P_m \end{cases} \quad (1)$$

corresponding to a *supersynchronous motor convention*, illustrated by Fig. 2 where

- ω_s is the stator frequency (rad/s),
- ω_r is the stator frequency (rad/s),
- Ω is the mechanical speed (rad/s),
- p is the number of pole pairs of the DFIM,
- P_s is the (entering) stator power,
- P_r is the (entering) rotor power,

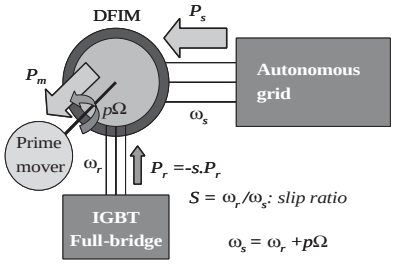

Fig. 2. Doubly-Fed Induction Machine in supersynchronous motor convention

- P_m is the (outgoing) mechanical power,
- s is the *slip ratio* defined as follows

$$s \triangleq \frac{\omega_r}{\omega_s} \quad (2)$$

In order to avoid all ambiguity between the two DFIM of the cascade, 1 and 2 subscripts will be employed for all quantities in the system. Then, several relations must be introduced to describe the rotor interconnections:

$$\omega_{r1} = \lambda_c.\omega_{r2} \quad (3)$$

where is the interconnection coefficient between the rotor windings, defined as follows

$$\lambda_c = \begin{cases} +1 \text{ for a direct coupling sequence} \\ -1 \text{ for an inverse coupling sequence} \end{cases} \quad (4)$$

and

$$P_{r1} = -P_{r2} \quad (5)$$

due to the same convention used for the two machines (*supersynchronous motor convention*) as it can be seen in Fig. 3.

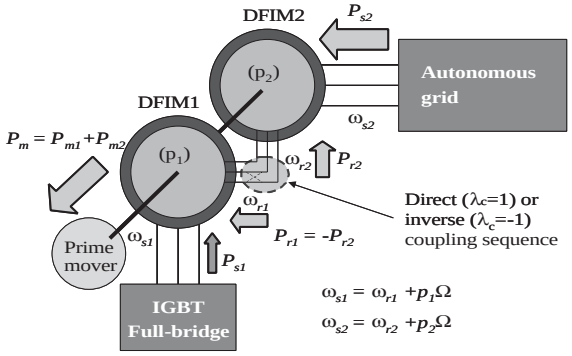

Fig. 3. Cascaded Doubly-Fed Induction Generator (CDFIG) power flow convention

All configurations have been studied in [8] and it has been shown that the inverse coupling sequence is the most interesting solution with $p_2 \geq p_1$. Notice that the test bench used in this paper is based on two DFIMs with the same number of pole pairs ($p_1 = p_2 = 2$).

IV. Dynamical modelling using dynamical equivalent circuits

A. Single DFIM dynamical model

A dynamical equivalent circuit of the doubly-fed induction machine can be easily deduced from dq equations of the machine in an arbitrary reference frame (stator reference frame here) as it is shown in Fig. 4. Notice that it describe the machine not only for steady-state operation but it is also valuable in transient mode operations. However, several components of the well-known steady-state equivalent circuit can be identified:

- magnetizing inductance, noted L_{cs},
- leakage inductance σL_{cr},
- ideal transformer (transformer turns ration m),
- and obviously, stator and rotor resistances, resp. R_s and R_r.

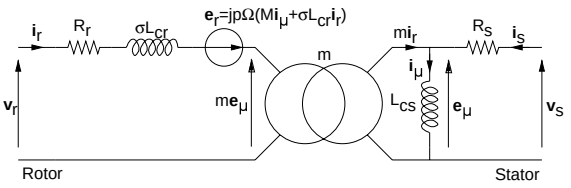

Fig. 4. Dynamical equivalent circuit representation of the Doubly-Fed Induction Machine (DFIM) in its stator *dq* reference frame

The electromechanical conversion is localized in the back e.m.f. $\underline{e}_r$. More precisely, this back e.m.f is composed of two terms

$$\begin{aligned} \underline{e}_r &= jp\Omega \left(M.\underline{i}_\mu + \sigma Lcr.\underline{i}_r \right) \\ &= \underline{e}_m + \underline{e}_{ar} \end{aligned} \tag{6}$$

where

- $\underline{e}_m = jp\Omega.M.\underline{i}_\mu$ is precisely the term which corresponds to the electromechanical conversion
- $\underline{e}_{ar} = jp\Omega.\sigma Lcr.\underline{i}_r$, which can be seen as an armature reaction e.m.f.

B. Rotor interconnection modelling

In the cascaded doubly-fed induction generator, two doubly-fed induction machines are connected by their rotor windings. As it has been presented in section III, the inverse coupling sequence has a real interest for generation systems applications.

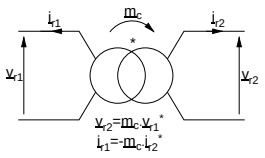

Fig. 5. Complex conjugate transformer introduced by the inverse coupling sequence between rotor windings of the CDFIG

Finally, a rotor interconnection model is proposed within this framework in Fig. 5. It is illustrated by an ideal transformer with a complex transformer turns ratio, noted $\underline{m}_c$ and defined as follows

$$\underline{m}_c\left(\theta\right) = e^{-j(p_1+p_2)\theta} = e^{-j\Sigma p\theta} \tag{7}$$

This transformer is also characterized by conjugate operations introduced in Fig. 5. This is why this transformer is called below *"complex conjugate transformer"*.

C. CDFIG model

Remark 1: For the CDFIG modelling, variables associated to DFIM1 and DFIM2 are distinguished by 1 and 2 subscripts.

An initial model based on a simple interconnexion of all the building blocks models be be directly established. However, the two rotor circuits of the DFIMs include two leakage inductances which are associated to the same state variable. Indeed, the rotor currents $\underline{i}_{r1}$ and i_{r2} are linked as it is shown in Fig. 5. Thus, it is mandatory to merge these two inductances into a single one which represents the global rotor leakage inductance of the CDFIG. Moreover, it can be noticed that it would be impossible to separate practically DFIM1 and DFIM2 leakages and only the global leakage inductance can be identified in such an integrated machine. On the basis of operations described in [8], this initial dynamical equivalent circuit is transformed into the one proposed in Fig. 6.

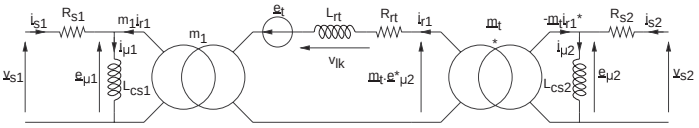

Fig. 6. CDFIG dynamical equivalent circuit

In this model, four new elements are introduced, defined as follows

$$R_{rt} = R_{r1} + R_{r2} \tag{8}$$

$$L_{rt} = \sigma_1 L_{cr1} + \sigma_2 L_{cr2} \tag{9}$$

$$e_t = j\Omega \left(p_1 M_1.\underline{i}_{\mu 1} + p_2 M_2.\underline{m}_c \underline{i}^*_{\mu 2} \right) - jp_1 L_{rt}\Omega.i_r \tag{10}$$

where $\underline{i}_r$ is the common rotor current in the merged rotor model of the CDFIG (notice that $\underline{i}_r = \underline{i}_{r1}$) and a global complex conjugate transformer with a complex transformer turns ratio noted $\underline{m}_t$ and defined as follows

$$\underline{m}_t = \underline{m}_c.m_2 \tag{11}$$

where m_2 is the (real) transformer turns ratio of DFIM2. On the basis of this graphical representation, main properties of the system are highlighted:

- System order: $n = 6$ (3 complex state variables $\underline{i}_{\mu 1}$, $\underline{i}_{\mu 2}$ and $\underline{i}_r$)
- Since θ and Ω are not considered as state variables but only parameters of this system, the CDFIG is a Linear Parameter Varying (LPV) system
- Two complex inputs are identified: $\underline{v}_{s1}$ and $\underline{v}_{s2}$
- Two complex outputs: $\underline{i}_{s1}$ and $\underline{i}_{s2}$

The dynamical equivalent circuit of the CDFIG is also translated into a block diagram as it is shown in Fig. 7 which can be implemented with Matlab/Simulink and used for simulations, allowing to validate theorically control strategies developped in section V.

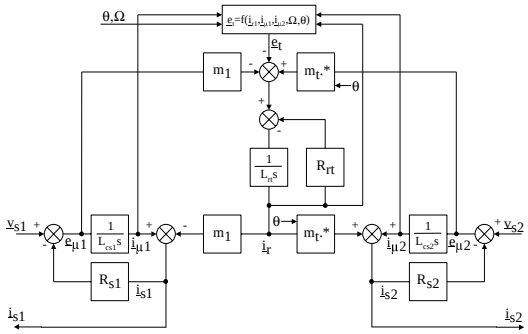

Fig. 7. Block diagram of the CDFIG (equivalent to 6)

D. Grid model and complete system

In the targeted application, the CDFIG is connected to an autonomous grid. In order to properly control grid voltages $\underline{v}_{s2}$, parallel capacitors are connected to the stator 2 windings of the CDFIG. Then, loads connected to this grid can be modelled using an equivalent current source as it is shown in Fig. 8.

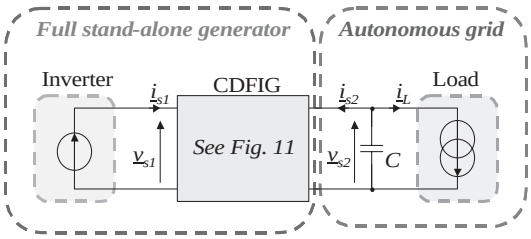

Fig. 8. Interconnexion between the CDFIG and the autonomous grid

Notice that model can take into account both linear and nonlinear loads and the grid voltage dynamics is characterized by the following equation:

$$\frac{d\underline{v}_{s2}}{dt} = -\frac{1}{C}\left(\underline{i}_{s2} + \underline{i}_L\right) \tag{12}$$

where $\underline{i}_L$ is the load(s) current.

Since the inverter connected to stator 1 windings is supposed to be an ideal voltage source, grid and CDFIG models are enough to describe the system behaviour. A global high level representation of the interconnexion between these two elements is proposed in Fig. 9.

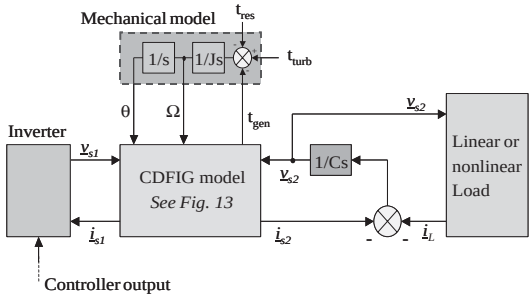

Fig. 9. Global model including the CDFIG and its load

Notice that the mechanical part of the system is included in this model but the generator torque t_{gen} can be neglected:

$$t_{gen} \ll t_{res} \tag{13}$$

thus, the mechanical speed and angle, respectively Ω and θ, do not depend on the electrical power consumed by the loads connected to the CDFIG. Thus, these two variables are considered as varying parameters of the CDFIG.

V. Controller synthesis

A. Principles of control using model inversion

The synthesis methodology proposed here is based on the *direct model* of the system presented above. Indeed, a controller can be seen as the inverse model of the plant to control [5],[6],[7].

B. CDFIG control overview

In the previous paragraph, it has been assumed that the output vector was equal to the state vector. In fact, in the CDFIG model, outputs correspond to measurable currents:

- stator 1 current $\underline{i}_{s1}$,
- and stator 2 current $\underline{i}_{s2}$,

whereas no state variables can be measured:

- magnetizing current $\underline{i}_{\mu 1}$,
- magnetizing current $\underline{i}_{\mu 2}$,
- rotor current $\underline{i}_r$.

A physical analysis of the CDFIG, on the basis of its dynamical equivalent circuit representation, leads to the following assessments:

- magnetizing current $\underline{i}_{\mu 1}$ and rotor current $\underline{i}_r$ cannot be controlled separately because they are associated to parallel branchs connected to a common voltage source (inverter) via a small resistance R_{s1}.
- as it is usually supposed, R_{s2} can be neglected and then, magnetizing current $\underline{i}_{\mu 2}$ is strongly coupled to the stator voltage $\underline{v}_{s2}$.

Thus, an overview of the CDFIG controller can be obtained with these two remarks:

- only one regulation loop has to be made for the rotor current $\underline{i}_r$ ($\underline{i}_{\mu 1}$ can be then considered as a slave variable),
- and this regulation loop is then controlled (with its reference) by an outer regulation loop dedicated to the output voltage regulation, as it is already done for a single doubly-fed induction generator in [9].

C. Rotor current estimation

As it has been established in the previous paragraph, the rotor current has to be controlled. However, this current is not measurable, this is why an estimator is required. A *simple open-loop estimator* is proposed here, based on the following expressions :

$$\begin{cases} \widehat{\underline{i}}_{\mu 1} = \frac{1}{L_{cs1}} \int \left(\underline{v}_{s1}^{meas} - R_{s1}\underline{i}_{s1}^{meas}\right).dt \\ \widehat{\underline{i}}_r = \frac{1}{m_1}\left(\widehat{\underline{i}}_{\mu 1} - \underline{i}_{s1}^{meas}\right) \end{cases} \tag{14}$$

where $\underline{v}_{s1}^{meas}$ and $\underline{i}_{s1}^{meas}$ are two measurements. Notice that CDFIG parameters (R_{s1}, L_{cs1} and m_1) are supposed to be identified.

D. Rotor current loop

On the basis of the inversion principle of dynamical models, rotor current state variable can be directly derived from the voltage applied to the rotor inductance L_{rt}. Thus, it can be noticed that

$$\underline{v}_{LRt} = m_t \underline{e}^*_{\mu 2} - m_1 \underline{e}_{\mu 1} - \underline{e}_t = L_{rt} \frac{d}{dt}[\underline{i}_r] + R_{rt} \underline{i}_r$$

ans $\underline{v}_{s1}$ is calculated in order to control $\underline{v}_{LRt}$ as shown in Fig. 10.

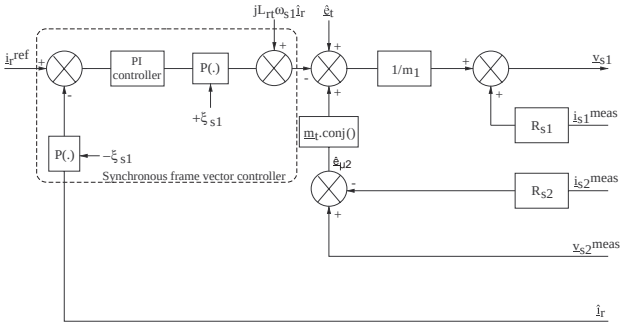

Fig. 10. Inner rotor current loop

Notice that $\underline{v}_{LRt}$ is the output of a *vector* PI controller. Using this strategy allows the cancellation of the compensation errors. Thereafter, the CDFIG controlled by this rotor current loop can be described with the help of a simplified model (Fig. 11). In this figure, $\widehat{\underline{e}}_{\mu 2}$ and $\widehat{\underline{e}}_t$ are estimation terms of values given in Eq. 10.

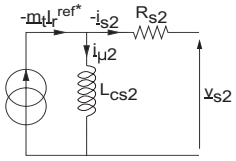

Fig. 11. {CDFIG + rotor current loop} equivalent circuit

E. Grid voltage regulation

The CDFIG is *not a natural voltage source*. So, parallel *capacitors are required* if a true voltage source is needed. Moreover, harmonic voltage disturbances are reduced because of their low impedance at high frequencies in comparison with the high impedance of the CDFIG (and its rotor current loop). The simplified dynamical equivalent circuit of the controlled generator and its load is presented Fig. 12. It includes:

- the CDFIG and its rotor current loop
- filtering parallel capacitors
- linear and/or nonlinear load described with an equivalent current source

An external loop has to be added in order to control the grid voltages. Notice that a magnetizing current $\underline{i}_{\mu 2}$ regulation is not required because this state variable *is strongly coupled* to the grid voltage $\underline{v}_{s2}$. If R_{s2} is neglected, it gives

$$\underline{v}_{s2} \approx \underline{e}_{\mu 2} \quad (15)$$

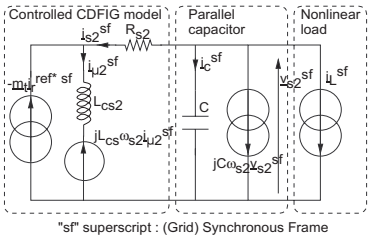

Fig. 12. Stator equivalent circuit in the field synchronous frame

Keeping in mind the inversion principle, the designed outer loop is presented Fig. 13.

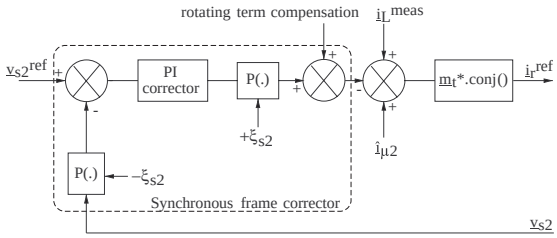

Fig. 13. Outer grid voltage loop

As shown in the next section, this strategy allows taking into account nonlinear loads.

VI. Simulations and experimental results

A. Testbench description

All the simulation parameters are given in TABLE I. They are based on the machines used in the testbench presented in Fig. 14.

TABLE I
TESTBENCH PARAMETERS

DFIMs parameters	DFIM 1	DFIM 2
Numbers of pole pairs	2	2
Rated power	2.2kW	4kW
Stator resistances	0.81Ω	1.67Ω
Rotor resistances	0.83Ω	0.25Ω
Stator cyclic inductances	138mH	296mH
Rotor cyclic inductances	20.9mH	21.1mH
Stator/Rotor mutual inductances	33.3mH	50.7mH
Coefficient of dispersion	0.117	0.077
Linear load parameters		
Resistance R	40Ω	
Inductance L	1mH	
Filtering capacitor C	1μF	

The simulation on utility grid uses an ideal model of the grid which is considered as a three-phase source voltage (230V, 50Hz).

B. Simulations

In a first simulation, the rotor current loop is tested at variable speed. Notice in Fig. 15 that during the acceleration (500tr/min/s), the rotor currents does not exactly follow its references.

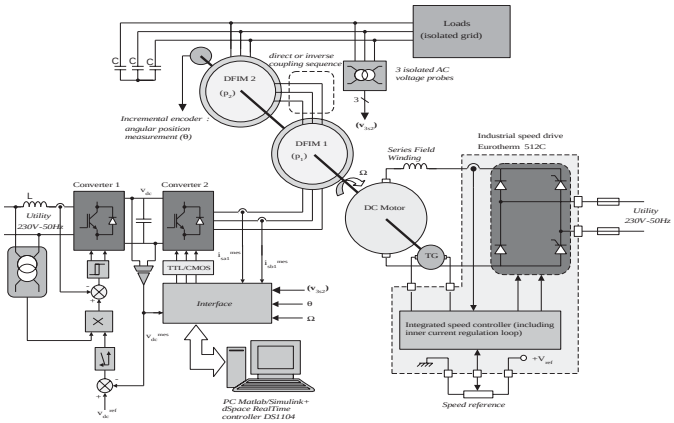

Fig. 14. Experimental testbench

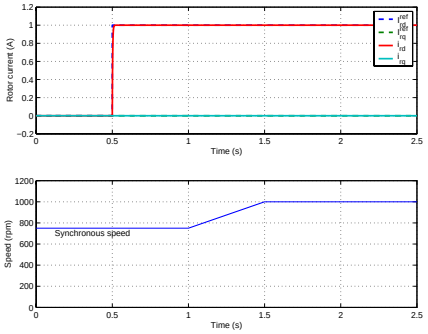

Fig. 15. Rotor current regulation at variable speed

In Fig. 16, the stator 1 currents and grid voltages are shown. We can see that the grid frequency is maintained equal to 50Hz in spite of the speed variations ($\pm 33\%$ of the synchronous speed). Thus, the VSCF operation is verified. Moreover, we can see that the stator 1 power is limited to a fraction of the grid power ($-P_{s2}$) for the whole speed range and is equal to zero at the synchronous speed.

C. Experiments

As it is shown in Fig. 17, sub. and supersynchronous operations correspond to a mechanical speed inferior and

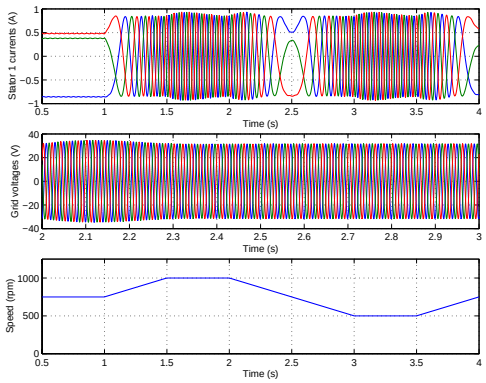

Fig. 16. VSCF control of the CDFIG

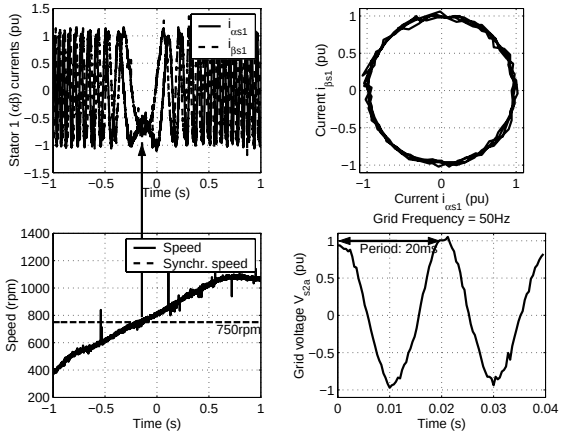

Fig. 17. Rotor currents (*i.e.* Stator 1 currents) regulation – Experimental results

superior to 750rpm resp. (for a grid frequency equal to 50Hz).

When the rotor currents control is achieved, grid voltage regulation can be performed, allowing to maintain voltage amplitude in spite of large variations of the load consumption.

VII. Conclusions

The cascaded doubly-fed induction machines studied in this paper have been successfully controlled as a variable speed constant frequency generator using a controller design methodology based on a user-friendly modelling formalism (dynamical equivalent circuit representations), adapted to electrical generation systems, which also allows to build the controller within a rigorous framework using inverse modelling principles.

References

[1] F. Runcos, R. Carlson, A. M. Oliveira, P. Kuo-Peng, N. Sadowski, *Performance Analysis of a Brushless Doubly-Fed Cage Induction Generator*, Nordic Wind Power Conference, Chalmers University of Technology, March 2004.

[2] S. Kato, N. Hoshi, K. Ogushi, *Small-scale hydropower*, IEEE Industry Applications Magazine, Vol. 9, No. 4, pp. 3-38, July-Aug. 2003.

[3] T. Ortmeyer, W. Borger, *Control of cascaded doubly-fed machines for generator applications*, IEEE Transactions on Power Appartus and Systems, Vol. PAS-103, No. 9, pp. 2564-2571, Sept. 1984.

[4] B. Hopfensperger, *Doubly-fed AC machines: classification and comparison*, in Proc. EPE'01, CD-ROM, Graz, Austria, Aug. 2001.

[5] G. Georgiou, B. Le Pioufle, *Combined magnetizing flux oriented control of the cascaded doubly-fed induction machine*, in Proc. EPE'91, Vol. 3, pg. 42,Firenze, Italy, 1991.

[6] J. P. Hautier, P. J. Barre, *The causal ordering graph – A tool for modelling and control law synthesis*, Studies in Informatics and Control Journal, Vol. 13, No. 4, pp. 265-283, Dec. 2004.

[7] A. Bouscayrol, M. Pietrzak-David, P. Delarue, R. Peña-Eguiluz, P.-E. Vidal, X. Kestelyn, *Weighted Control of Traction Drives With Parallel-Connected AC Machines*, IEEE Trans. on Industrial Electronics, Vol. 53, No. 6, pp. 400-408, Dec. 2006.

[8] N. Patin, J.-P. Louis, E. Monmasson, *Cascaded doubly-fed induction generator - State-space modelling and performance analysis*, in Proc. Electrimacs'05 Conf., CD-ROM, Hammamet, Tunisia, 17-20 Apr. 2005.

[9] N. Patin, E. Monmasson, J.-P. Louis, Control of a stand-alone variable speed constant frequency generator based on a doubly-fed induction machine, in EPE Journal, Vol. 16, No. 6, pp. 37-43, Dec. 2006.